J Therm Anal Calorim (2013) 111:499–506
DOI 10.1007/s10973-012-2536-7

Red phosphorus acts as second acid source to form a novel intumescent-contractive flame-retardant system on ABS

Hai-qing Yin · Dan-dan Yuan · Xu-fu Cai

Received: 9 April 2012 / Accepted: 4 June 2012 / Published online: 3 July 2012

Abstract A novel halogen-free flame retardant prepared by poly(*p*-ethylene terephthalamide) and ammonium polyphosphate (APP) on acrylonitrile–butadiene–styrene (ABS) resin has a good flame retardancy when loading is 30 %; but, once the mass fraction is <30 %, the system does not maintain outstanding flame retardancy. To improve the efficiency of this kind of flame retardant and LOI values, higher thermal stability acid source-red phosphorus is introduced. It is found that a little quantity of red phosphorus will improve the flame retardancy of ABS remarkably and will change the process of charring; when the mass fractions of APP, PPTA, and red phosphorus are only 15, 5, and 2 %, respectively, though the LOI of flame-retardant ABS is 27, UL-94 vertical burning test still reach V-0. Thermogravimetric analysis data show that red phosphorus changes the thermal degradation behavior of IFR-ABS system, shrink digital photo display system, and yield more stable residue at higher temperature; Fourier transform infrared results and scanning electron microscopic micrographs show that red phosphorus can catalyze the charring and form much denser char to improve the flame-retardant performance of the materials.

Keywords Red phosphorus · ABS · Second acid source · Intumescent-contractive flame retardant · Synergistic

H. Yin · D. Yuan · X. Cai (✉)
Department of Polymer Science and Materials, The State Key Laboratory of Polymer Materials Engineering, Sichuan University, Chengdu 610065, China
e-mail: caixf2008@scu.edu.cn

Introduction

Acrylonitrile–butadiene–styrene (ABS) is a widely used thermoplastic material because of its good mechanical properties, chemical resistance, and processing advantages. However, easy combustibility and melt dripping limit its applications. In many applications, it is necessary to construct a flame-retarded composition for ABS resin [1].

The common flame retardants for ABS were halogen-containing compounds. Bromine-containing compounds, such as decabromodiphenyl oxide, tetrabromobisphenol, etc., are very effective and show a good ratio of property to price in flame retardancy of ABS resin [2], but the use of these flame retardants has been limited for the consideration of life safety and environmental problems. Consequently, it is essential that new flame-retardant systems should be developed to meet the constantly changing demand of new regulations, standards, and test methods

In recent years, intumescent flame retardant (IFR) with particular char-yielding properties have been widely used in various polymeric materials [3–7] is well known as a new generation of flame retardants in ABS and other polyolefin for some of their merits, such as very low smoke and toxic gases produced during burning, and antidripping property, which conform to the tendency of flame retardants' development. However, it has also some flaws compared with bromine-containing flame retardants [8, 9], such as low flame-retardant efficiency. In order to enhance the effective of flame retardancy, new intumescent flame-retardant systems have been found [10–15], and synergistic agents have been used in IFR systems, such as zeolites [16, 17] and some transitional metal oxides and metal compounds [18]. Many researches have shown that synergistic agents can effectively promote in catalyzing the reactions among IFR components in IFR-ABS systems.

In previous work, many halogen-free flame retardancy systems need high loading to get perfect flame retardancy, such as PETA/APP system needs 30 % and many synergistic agents only improve flame retardancy on foundation, which means they cannot reduce the loading of flame-retardant meantime gain perfect flame retardancy. In this work, high thermal stability acid source—red phosphorus—is selected as second acid source to makes up the deficiency of single acid source in an effective IFR system consisting of ammonium polyphosphate (APP) and a char-foaming agent [poly (*p*-ethylene terephthalamide)] (PETA) to assemble a novel system. The new system has two charring processes, including swell and shrink. Limiting oxygen index (LOI), vertical burning test (UL-94), thermogravimetry analysis (TG), Fourier transform infrared (FTIR), and scanning electron microscopy (SEM) are used to evaluate the synergistic effect and study synergistic mechanism of red phosphorus in ABS-IFR systems.

Experimental

Materials

ABS copolymer (0215-A) is supplied by Jilin Petrochemical Co. (Jilin, China). APP is obtained from Zhejiang Longyou GD Chemical Industry Corp. (Longyou, China). Terephthaloyl chloride (TPC) is supplied by Shanghai Xinliang Chemical Reagent Factory (Shanghai, China). 1,2-ethylenediamine, calcium chloride ($CaCl_2$), red phosphorus, triethylamine, and *N*,*N*-dimethylacetamide (DMA) are purchased from Kelong Chemical Reagent Corp. (Chengdu, China).

Instrumentation

All TG tests are carried out using a Perkin Elmer Pyris 1Thermal Analyser at a linear heating rate of 10 °C min^{-1} under pure nitrogen within the temperature range from 50 to 800 °C. The mass of the samples is kept within 8–10 mg. All data can be seen in the TG and DTG thermographs. ^1H NMR (400 Hz) spectra are recorded on a FT-80A NMR using CF_3COOD as a solvent. The FTIR spectra of the char residues are recorded on a Nicolet MAGNA-IR 560 spectrometer by a KBr plate technique. The surface morphology of the char obtained after the LOI test is observed using Inspect-F SEM.

The flame retardancy of all samples is characterized by LOI and UL-94 methods. LOI data of all samples are obtained at room temperature on an oxygen index instrument (XYC-75) produced by Chende Jinjian Analysis Instrument Factory, according to GB/T2406-93 standard. The dimensions of all samples are 130 × 6.5 × 3 mm. LOI is an important parameter for evaluating the ease of extinguishment of polymeric materials in the same condition. It denotes the lowest volume concentration of oxygen sustaining candle burning of materials in the mixing gases of nitrogen and oxygen. Vertical burning rates of all samples are measured on a CZF-2 instrument produced by Jiangning Analysis Instrument Factory, with sample dimensions of 125 × 12.5 × 3.2 mm, according to UL-94 test ASTM D635-77. UL-94 test results are classified by burning ratings V-0, V-1or V-2.

Synthesis of PETA (Scheme 1)

A 250-mL three-necked round bottom flask equipped with a stirrer is charged with 5.4 g $CaCl_2$, 4.8 g (0.08 mol) 1,2-ethylenediamine, and 180 mL DMA. Then the mixture is stirred and when the $CaCl_2$ dissolved completely, the flask is cooled to 0–5 °C. After that, 16.24 g (0.08 mol) TPC is added slowly to the flask within about 0.5 h. 1 h later, 16.18 g (0.16 mol) triethylamine is added slowly when the reaction temperature is kept at 0–10 °C. Then, the flask is heated up to 45–50 °C and the reaction will be completed after 4 h; the reaction mixture is cooled to room temperature and then the mixture is poured into distilled water and filtered. The white solid is washed with water and dried in a vacuum oven at 100 °C to constant mass. The yield is 16.8 g (79.8 %)

Sample preparation

New IFR consist of APP, PETA, and red phosphorus. The ratio of APP to PETA is fixed at 3:1, and a loading of red phosphorus is kept at 0, 1, 2, 3, 4 wt% in the IFR. The ABS and IFR systems are mixed in an HAAKE plasticorder mixer at 195 °C and 50 rpm for 8 min. The mixed samples are transferred to a mold and preheated at 200 °C for 3 min, then pressed at 10 MP, and successively cooled to room temperature while maintaining the pressure to obtain the composite sheets for further measurements. Before mixing, all the components are dried in an oven at 80 °C for 12 h.

Results and discussion

Characterization of PETA

Figure 1a presents the FTIR spectra of the synthesized PETA. The absorption bands at 1,541, 1,497, and 3,072 cm^{-1} corresponded to vibrations of the benzene rings, and the peaks at 2,976 and 2,932 cm^{-1} are assigned to $–CH_2$ band. The absorptions at 1,636 and 3,293 cm^{-1}

Scheme 1 Synthesis of PETA

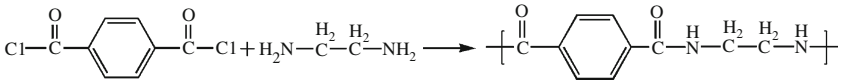

are associated with the stretching mode of C=O and N–H from the acrylamide group, respectively.

The ^{1}H NMR spectra of PETA are shown in Fig. 1b. The peak at $\delta = 7.58$ ppm is assigned to aromatic protons. The peak around $\delta = 3.61$ ppm corresponded to the $-CH_2$ protons. The absorption of –NH proton may be covered by a solvent for there is proton-changing reaction happens between them. All the information above confirms that the target product is synthesized successfully.

Flammability properties

The effect of IFR-ABS composites without and with red phosphorus is shown in Table 1. The LOI value of the IFR-ABS composite without red phosphorus is 30 and UL-94 test reaches V-0 when the quantity of the IFR consisted of PETA and APP is 30 wt % (the proportion of system is consult previous work of our lab); however, once the mass fractions lower than 30 %, like 25 %, it do not pass UL-94 test and LOI value decrease to 25. From later part of Table 1, it can be seen that the effect of red phosphorus is so remarkable and it mainly reflects at low loading; when the quantity of APP/PETA are 25 wt% and 20 % with 2 wt% red phosphorus appended, it can reach V-0 all the same and LOI value are 30 and 27. The increased degree is larger than high loading, this may because the effect of APP/PETA is perfect when mass fraction is 30 %, as the loading decrease to 25 %, these is not enough charring layer to isolate fire, while red phosphorus can strengthen the charring layer, hence the effect looks like so remarkably. It can be seen that the increased LOI values are not very obvious with the change of quantity of red phosphorus when the mass fractions of IFR is 30 %, with 1, 2, 3, 4, and 5 % red phosphorus appended, respectively, LOI value of IFR-ABS composites is 31, 32, 32, 33, and 32. It shows that the loading of red phosphorus reaches 4 %, LOI got maximum value of 33, and with the further increase red phosphorus in IFR, the LOI values decrease. This may be because red phosphorus is flammable; when temperature is high, it will release heat. When 5 wt% of red phosphorus is added, red phosphorus releases too much heat inside composites to break char layer so it does not increase LOI value after 4 wt% [18]. The results of LOI and UL-94 tests indicated that red phosphorus is a superduper synergistic agent, and taking account of 4 % loading do not improve flammability properties and the mechanical property of material remarkably; we choose formulation 4 (2 % red phosphorus) to do further study.

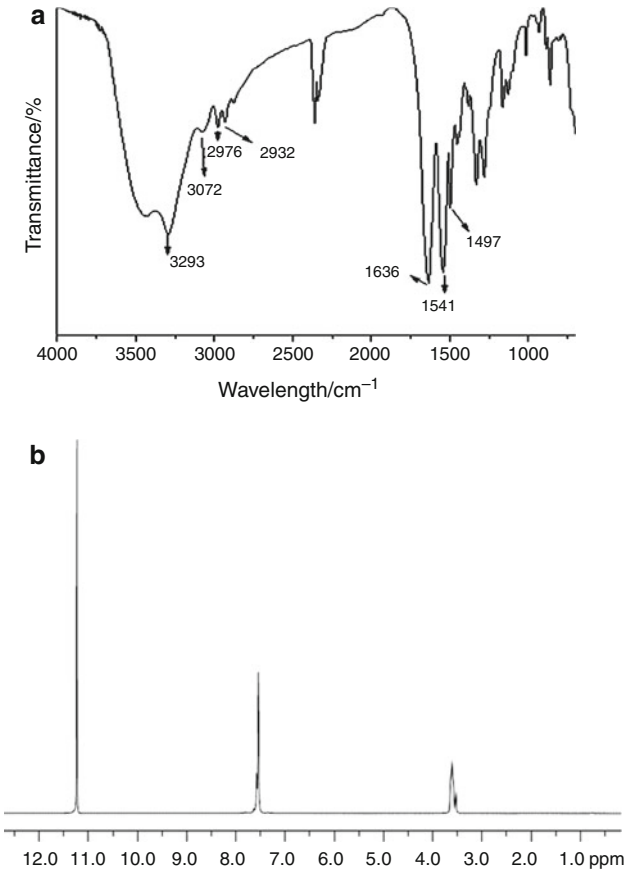

Fig. 1 FTIR spectrum and ^{1}H NMR spectrum of PETA

Thermal analysis

In order to further investigate the synergistic effect between APP/PETA system and red phosphorus, thermal properties are compared. Figure 2a shows the TG curves of the IFR system with and without red phosphorus and the data are listed in Table 2. In Fig. 2a, the influence of red phosphorus on the thermal degradation of the IFR is shown; it can be seen that the thermal degradation behavior between IFR and IFR-red phosphorus presents a clear difference, especially focus on the range of high temperature. Before 500 °C, two curves almost have the same trend; this result shows that red phosphorus does not promote decomposition of APP and PETA. After 500 °C, the trend of curve stand for IFR-red phosphorus decline suddenly; it should be the influence of second acid source—red phosphorus produces phosphorous compound to promote further charring [19], which obviously reflects at DTG curves (Fig. 2b); the thermal decomposition temperature of the third mass loss peak of IFR system

Table 1 The flame retardancy of IFR-ABS systems without and with red phosphorus

Sample	Components/mass%				LOI	UL-94
	ABS	APP	PETA	Red phosphorus		
1	70	22.5	7.5	–	30	V-0
2	75	18.75	6.25	–	25	Failure
3	70	22.5	7.5	1	31	V-0
4	70	22.5	7.5	2	32	V-0
5	70	22.5	7.5	3	32	V-0
6	70	22.5	7.5	4	33	V-0
7	70	22.5	7.5	5	32	V-0
8	75	18.75	6.25	2	30	V-0
9	80	15	5	2	27	V-0

decreased from 618 to 553 °C and has a extra peak at 505 °C which may brought by the loss of red phosphorus. This fact illuminates that red phosphorus changes the thermal degradation behavior of APP-PETA system and it makes system complete the charring process at lower temperature; this effect makes working temperature of flame retardants more close to the decomposition temperature of ABS resin. Moreover, red phosphorus does not improve mass of char residue clearly, for instance, the char residue of the IFR without red phosphorus is 51 wt% at 600 °C and 37 wt% at 700 °C, while that of the IFR system with 2 wt% red phosphorus is 43 and 38 wt%, respectively. However, from these data, it testifies that red phosphorus catalyze carbonization process at lower temperature and make char residue more stable; this due to the work of red phosphorus to create more P=O band and then there are more crosslink bands [20] after the reaction of APP, the second crosslinks reinforce the char layer.

Figure 3 and the latter part of Table 2 give the thermal degradation curves and data for ABS and IFR-ABS composites without and with 2 % red phosphorus. The IFR is fixed at 30 wt% in all samples. Unlike the virgin ABS almost showing one sharp decomposition at 415 °C (Fig. 3a), and nearly no char residue left over 600 °C, the thermal degradation behavior of the ABS-IFR composite is different from that of ABS; the flame retardant clearly decreases the $T_{initial}$ of the ABS resin nearly to 50 °C; however, the accession of red phosphorus in IFR system displays little influence on the $T_{initial}$ of the ABS-IFR composites. From Table 2 and Fig. 3b, the DTG curve shows that T_{max} of ABS-IFR and ABS-IFR-red phosphorus is also close, all round 400 °C; the weakened peak shows that the flame retardants slow down the decomposition rate of material. This data demonstrate that char layer prolongs the thermal decomposition process of ABS and 2 % red phosphorus will not change decomposition behavior of ABS-IFR composites clearly; however, a little increased mass of char layer illuminates that red phosphorus can promote char formation of the ABS-IFR composites.

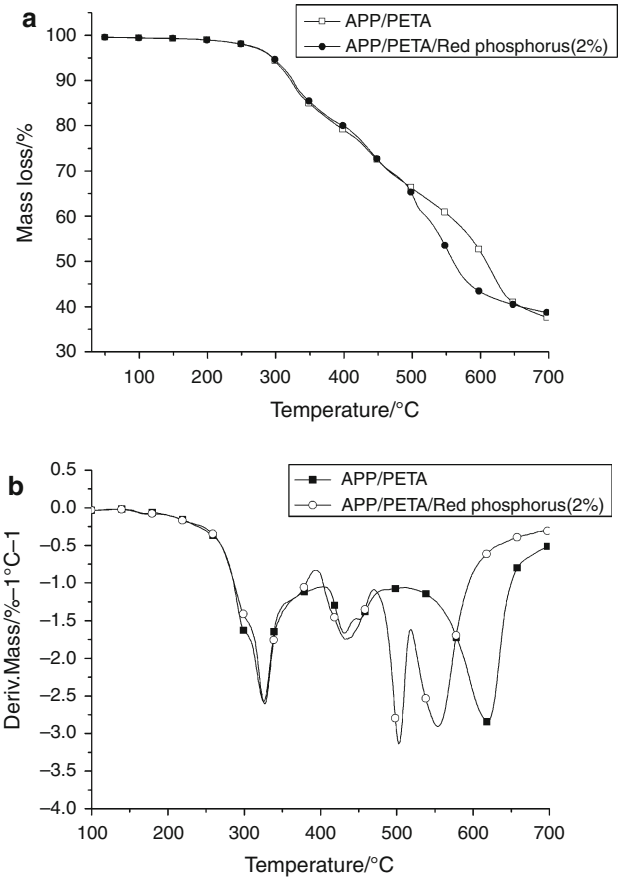

Fig. 2 TG and DTG curves of IFR with and without red phosphorus in N_2

Char-forming mechanism

For the sake of elucidating how the formation of intumescent char affects the combustion of the flame-retarded ABS composites and whether there be difference after red

Table 2 TG and DTG data of thermal degradation of system and char residue

Sample	$T_{initial}$/°C	T_{max}/°C	Char residue/%		
			500/°C	600/°C	700/°C
APP/PETA/(2 %) red phosphorus	295	553	64	43	38
APP/PETA	290	618	66	51	37
ABS	378	415	8	2.5	–
Formulation 4 (30 %)	329	400	30	18	5
ABS/APP/PETA (30 %)	340	404	28	19	3

$T_{initial}$ the initial decomposition temperature (based on 5 % weight loss)

T_{max} the max-rate degradation temperature

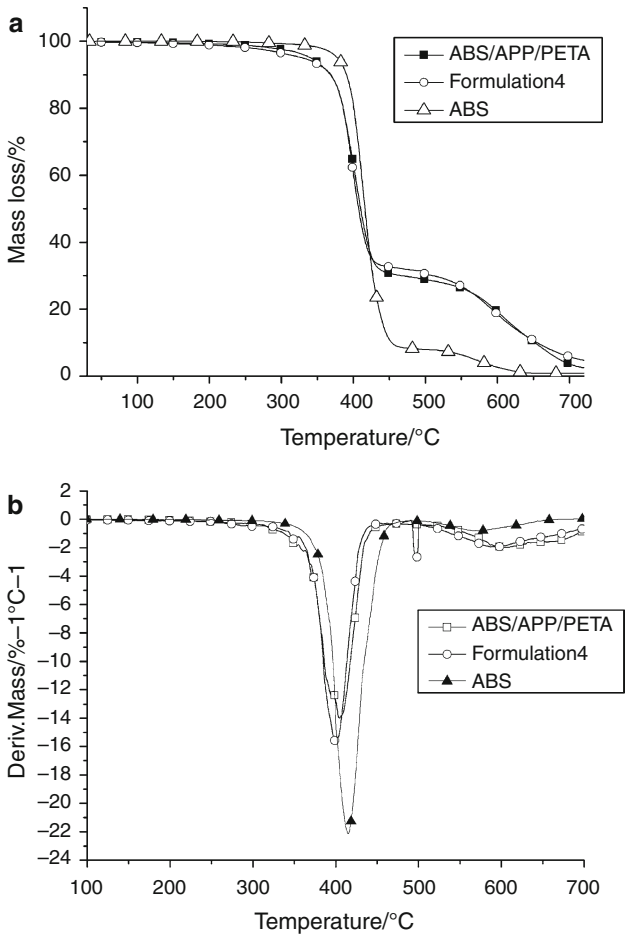

Fig. 3 TG and DTG curves of ABS-IFR with and without red phosphorus in air

phosphorus is introduced or not, the structures of residues left after the LOI test are examined by FTIR spectra and the microstructures of the char after combustion are investigated by SEM.

Figure 4a, b displays the FTIR spectrum of the residue of APP/PETA/Red phosphorus and APP/PETA system at different temperatures, including 25, 350, 450, and 550 °C. Comparing the spectra of these two groups, it shows the same process in main because there are no new bands yielded during this process, which means employed red phosphorus will not change the main mechanism. According to the strong band at 2,387 cm^{-1}, which should belong to cumulative double bonds N=C=O produced by the decomposition of polyacrylamide and P=O band of APP around 1,250 cm^{-1} disappear at 350 °C, the reaction of flame retardant for single APP at 350 °C still has P=O; this process should be the first part and the residue produced by this process is important to the charring process. As temperature was kept rising, cumulative double bonds form N=C=N groups and generate CO_2 through dimerization to isolate heat and then to crosslink with phosphorous compound which yielded by APP at higher temperature (like 450 °C) because P=O bands appear again and the absorption has a little excursion; this should be the second charring process [21]. While at 350 °C, these two spectra have a little distinction. At this temperature, in the system with red phosphorus, there is band absorption at 1,253 cm^{-1} belonging to P=O, which is produced by red phosphorus; however, this band almost disappears in APP/PETA system at 350 °C; this fact indicates that the reaction between PETA and APP is almost over at 350 °C. Meanwhile, the absorption at 1691, 1512, and 1,485 cm^{-1} are assigned to the C=O and characteristic absorption band of benzene skeleton vibration, which indicates that system still has acid amide (PETA) when most APP is done; this is to say that single acid source will not lead decomposition of PETA completely and red phosphorus will make up the deficiency. Spectrum of the residue of two systems at 450 is the same, but absorption area of APP/PETA/RP system is bigger. APP/PETA/RP system has red phosphorus so the first part process at lower temperature is more sufficient than the system without red phosphorus; the charring process at high temperature is faster for red phosphorus provides more phosphorus compounds. Figure 4c shows the residue spectrum of two systems at 550 °C; there is no obvious distinction except the absorption area, and this absorption almost likes spectrum of the residue after LOI

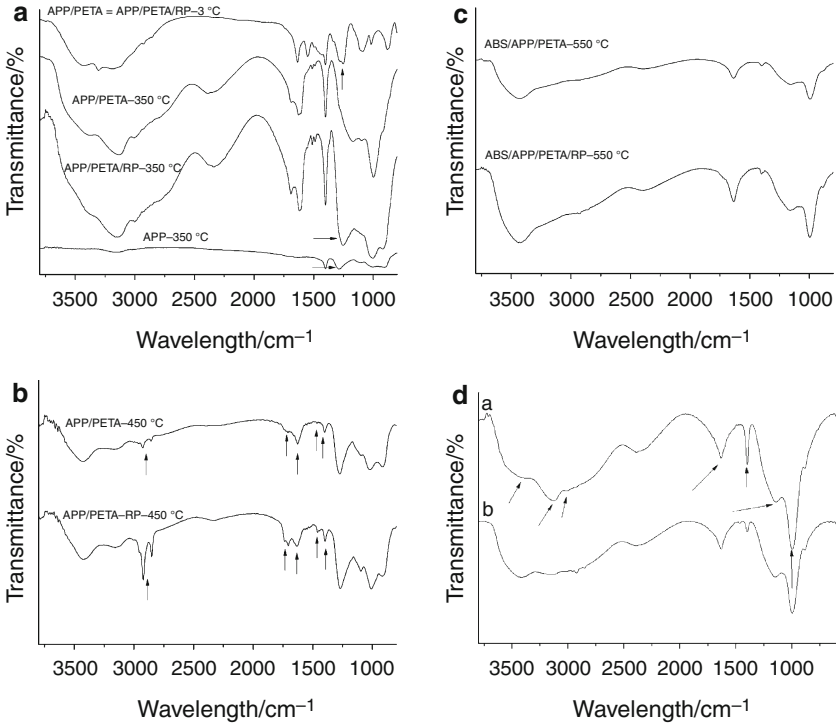

Fig. 4 FTIR spectrum of the residue of IFR with and without red phosphorus

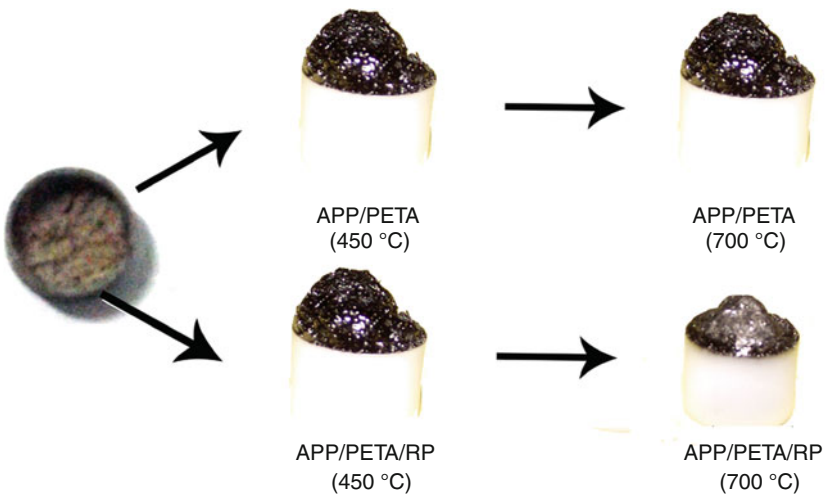

Fig. 5 Swell and shrink process of flame retardant system

test, which means that the reaction is coming to the end and there is mainly charring process at this temperature.

Figure 4d shows the FTIR spectrum of the residue obtained from LOI test of IFR-ABS with and without red phosphorus at different temperatures. As can be seen, there is no clear distinction between IFR and IFR-red phosphorus system. The absorption band at 3,417 cm^{-1} is assigned to the stretching mode of –OH from the P–OH group, and the band at 3,128 and 1,634 cm^{-1} correspond to the stretching mode of N–H in NH_4^+ and C=C stretching or poly-aromatics, respectively [22]. The absorption band at 1,151 cm^{-1} is attributed to P–O–C structure in P–C complex, and the peak around 1,000 cm^{-1} is for the symmetric vibration of P–O bond in P–O–C group [23]. Meanwhile, it is noticed that the bands at 2922, 2851, and 1,400 cm^{-1} are due to the organic species in the residues [24]. The FTIR spectra confirm that both P–O–P and P–O–C structural groups are present in charred layers, which indicate that the crosslinking reaction between PPTA and APP occur and red phosphorus will not change that mechanism.

The major characteristic of an intumescent coating is its ability to swell. This parameter is necessary, but not enough to insure fire protection because the char formed may be too light and not sufficiently mechanically resistant. Two acid source systems accord with this concept; at lower temperature, system can swell well and at higher

temperature it shrinks. In the meantime, it loses some residue, which has worse strength; thus, the charring layer left becomes better. The structure having a relatively strong charred layer is more important to minimize the heat transfer and provide good protection for the substrate [25]. Figure 5 shows the changed process of APP/PETA and APP/PETA/Red phosphorus systems. At room temperature, it is powders at 450 °C system swelled visibly, and at this moment red phosphorus did not finish its work, but blended in the residue. As the temperature rises continuously, red phosphorus produces more phosphate compounds, which promote more dehydration of acidamide inside the residue; this process provides more crosslink bands to make residue shrink at high temperature, and in the meantime loses some weak char residue. The char layer under two processes at 700 °C is obvious and more compact than that at 450 °C. However, only system without red phosphorus has one process of charring from 450 to 700 °C.

Figure 6a, b are SEM micrographs of the char residue of IFR-ABS composites without and with red phosphorus after LOI test at 30 % loading, respectively. Figure 6a shows micrographs of the char residues of ABS with APP/PETA. Obviously, char residues have lots of small holes and is not very condensed; this structure does not isolate heat and oxygen perfectly. Figure 6b stands for IFR systems containing red phosphorus; it can be seen that char residue under two processes has no flaws and becomes more tight; this structure can better prevent the oxygen and transfer heat between the flame zone and the substrate, thus protecting the underlying materials from further burning and pyrolysis.

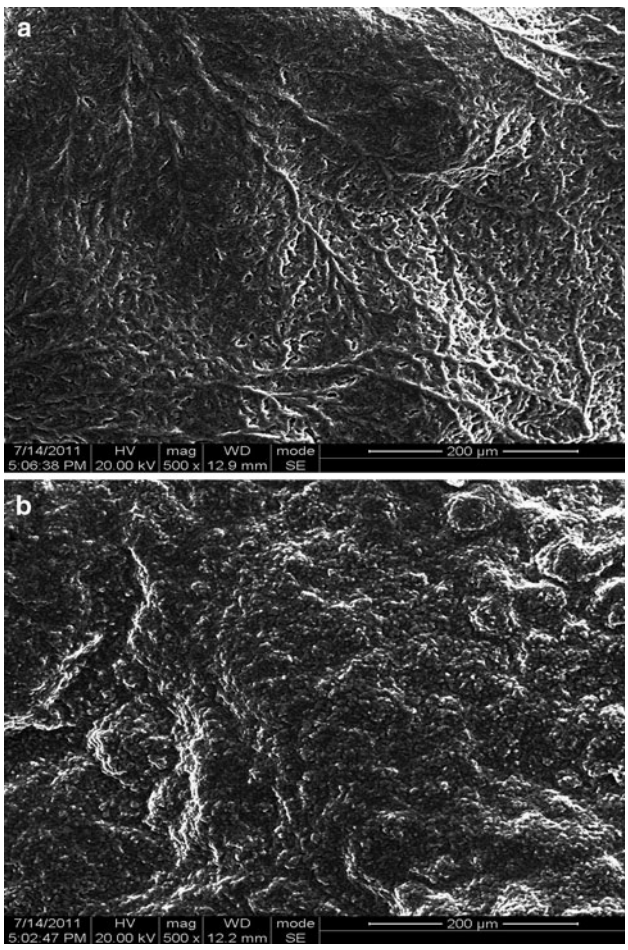

Fig. 6 SEM micrograph of char residue of ABS-IFR with and without red phosphorus: **a** ABS/APP/PETA (30 %), ×500; **b** ABS/APP/PETA/red phosphorus (30 %), ×500

Conclusions

A novel high performance IFR-ABS-Red phosphorus formulation is suggested, satisfying UL-94V-0 rating (3.2 mm), and LOI value reaches 27 in the case of IFR (20 wt%) and 2 wt% red phosphorus; it is more efficient compared with single acid source IFR system which needs 30 % loading to make ABS as good flame retardant. Considering the high melting point of PETA and the decreased loading, this flame retardant is a potential additive to improve flame retardancy, and in the meantime improve the impact strength when the size of system is close to nanometer, based on theory of rigid particle toughening. According to the TG curves, though the incorporation of red phosphorus into IFR (APP + PETA) hardly influence on charring mass of ABS formulations, it accelerates the process of yield stability residue (Fig. 2) to isolate fire. Residual chars contain polyphosphoric or phosphoric acid, which plays an important role in the process of carbonization, which is observed by FTIR spectrum in this system; it shows that red phosphorus does not change the process and mechanism, but the second acid source gives the system the second chance to yield thermal stability compound because red phosphorus can offer more phosphorus to form crosslink bands which can reinforce the strength of char residue. The morphological structure of char residue proves that the addition of red phosphorus makes system the produce more compact and homogeneous char on the surface, which is the most important part for the flame-retardant performance.

References

1. Wang SF, Hu Y, Zong RW, Tang Y, Chen Z, Fan WC. Preparation and characterization of flame retardant ABS/montmorillonite nanocomposites. Appl Clay Sci. 2004;25(1):49–55.
2. Brebu M, Bhaskai T, Murai K, Muto A, Sakata Y, Uddin MA. The individual and cumulative effect of brominated flame retardant and polyvinylchloride (PVC) on thermal degradation of

acrylonitrile–butadiene–styrene (ABS) copolymer. Chemosphere. 2004;56:433–40.
3. Le Bras M, Bugajny M, Lefebvre J, Bourbigot S. Use of polyurethanes as char-forming agents in polypropylene intumescent formulations. Polym Int. 2000;49:1115–24.
4. Zhu WM, Weil ED, Mukhopadhyay S. Intumescent flame-retardant system of phosphates and 5,5,5′,5′,5″,5″-hexamethyltris(1,3,2-dioxaphosphorinanemethan) amine 2,2′,2″-trioxide for polyolefins. J Appl Polym Sci. 1996;62(13):2267–80.
5. Xie RC, Qu BJ. Expandable graphite systems for halogen-free flame-retarding of polyolefins. I. Flammability characterization and synergistic effect. J Appl Polym Sci. 2001;80(8):1181–9.
6. Ma ZL, Zhang WY, Liu XY. Using PA6 as a charring agent in intumescent polypropylene formulations based on carboxylated polypropylene compatibilizer and nano-montmorillonite synergistic agent. J Appl Polym Sci. 2006;101:739–46.
7. Xu JZ, Jiao YH, Zhang B, Qu HQ, Yang GZ. Tin dioxide coated calcium carbonate as flame retardant for semirigid poly (vinyl chloride). J Appl Polym Sci. 2006;101:731–8.
8. Camino G, Grassie N, McNeill IC. Influence of the fire retardant, ammonium polyphosphate on the thermal degradation of poly (methyl methacrylate). J Polym Sci Polym Chem Ed. 1978;16: 95–106.
9. Li B, Sun CY, Zhang C. An investigation of flammability of intumescent flame retardant polyethylene containing starch by using cone calorimeter. Chem J Chin Univ. 1999;20(1):146–9.
10. Li B, Xu MJ. Effect of a novel charringefoaming agent on flame retardancy and thermal degradation of intumescent flame retardant. Polym Degrad Stab. 2006;91:1380–6.
11. Allen David W, Edwyn C. Structure–property relationships in intumescent fire retardant derivatives of 4-hydroxymethyl-2,6,7-trioxa-1-phosphabicyclo [2,2,2] octane-1-oxide anderton. Polym Degrad Stab. 1994;45:399–408.
12. Hu XP, Li YL, Wang YZ. Synergistic effect of the charring agent on the thermal and flame retardant properties of polyethylene. Macromol Mater Eng. 2004;289:208–12.
13. Almeras X, Dabrowski F. Using polyamide 6 as charring agent in intumescent polypropylene formulations. II. Thermal degradation. Polym Degrad Stab. 2002;77:315–23.
14. Liu Y, Yi JS, Cai XF. The investigation of intumescent flame-retarded polypropylene using poly(hexamethylene terephthalamide) as carbonization agent. J Therm Anal Calorim. 2012;107: 1191–7.
15. Zhang Q, Cheng YH. Synergistic effects of ammonium polyphosphate/melamine intumescent system with macromolecular char former in flame-retarding polyoxymethylene. J Therm Anal Calorim. 2011;18:293–303.
16. Demir H, Arkıs XE, lkü SÜ. Synergistic effect of natural zeolites on flame retardant additives. Polym Degrad Stab. 2005;89: 478–83.
17. Bourbigot S, Le Bras M, Delobel R, Bre'ant P, Tremillon J-M. 4A zeolite synergistic agent in new flame retardant intumescent formulations of polyethylenic polymers e study of the effect of the constituent monomers. Polym Degrad Stab. 1996;54:275–87.
18. Wang ZZ, Jiao CM, Hu KL. Properties of the thermal decomposition of hydrotalcite/red phosphorus flame retardant on EVA material. Polym Mat Sci Eng. 2009;25(9).
19. Estevao LRM, Le Bras M, Delobel R, Nascimento RSV. Spent refinery catalyst as a synergistic agent in intumescent formulations: influence of the catalyst's particle size and constituents. Polym Degrad Stab. 2005;88:444–55.
20. Liu CS, Wang Q. Morphology and mechanical properties of PP-g-HMA compatibilizer PA6/PP/wollastonite composite prepared by mechanochemical. Chin Plast Ind. 2000;30(4).
21. Wang J, Lu CX, Ren XC, Cai XF. J SiChuan Univ. 2010;42(2).
22. Wang DY, Cai XX, Qu MH, Liu Y, Wang JS, Wang YZ. Preparation and flammability of a novel intumescent flame-retardant poly(ethylene-*co*-vinyl acetate) system. Polym Degrad Stab. 2008;93:2186.
23. Mahapatra SS, Karak N. *s*-Triazine containing flame retardant hyperbranched polyamines: synthesis, characterization and properties evaluation. Polym Degrad Stab. 2007;92(6):947.
24. Camino G, Sgobbi R, Zaopo A, Colombier S, Scelza C. Investigation of flame retardancy in EVA. Fire Mater. 2000;24:85.
25. Jimenez M, Duquesne S, Bourbigot S. Multiscale experimental approach for developing high-performance intumescent coating. Ind Eng Chem Res. 2006;45(13):4500.